Application of Deep Learning to Seismic Event Classification in the Gujarat Region, India

D. Pragnath [1,3], G. Srijayanthi [1, *], Johannes Faber[2,4], Jonas Köhler[2,4], Wei Li[2],

Nishtha Srivatsava [2,4], Santosh Kumar [1], Sumer Chopra [1]

The supplementary information file contains 2 tables and 9 figures.

Table S1: Accuracy and loss function with varying batch sizes of waveform model. The bold text indicates the best accuracy.

Learning rate	***Batch size***	***Accuracy***	***loss***	***Early stop epochs***
10^{-4}	4	95.61	0.1123	73
10^{-4}	8	95.52	0.1193	122
10^{-4}	16	94.90	0.1425	64
10^{-4}	32	94.64	0.1456	68
10^{-4}	64	94.60	0.1584	100
10^{-4}	128	94.20	0.1711	73
10^{-4}	256	93.50	0.1962	94
2×10^{-4}	4	90.51	0.2980	70

2×10^{-4}	8	92.69	0.1829	71
2×10^{-4}	**16**	**95.32**	**0.1274**	**64**
2×10^{-4}	32	93.57	0.1798	36
2×10^{-4}	64	95.03	0.1304	100
2×10^{-4}	128	94.22	0.1621	52
2×10^{-4}	256	94.26	0.1682	65

Table S2: The Area Under the Curve (AUC) obtained for waveform (WF), spectrum (SPEC) and combined (COM) models for individual classes.

AUC	**Waveform**	**Spectrum**	**Combined**
Overall	0.98	0.93	0.98
Blast	0.98	0.92	0.98
Earthquake	0.97	0.90	0.97
Noise	0.99	0.96	0.99

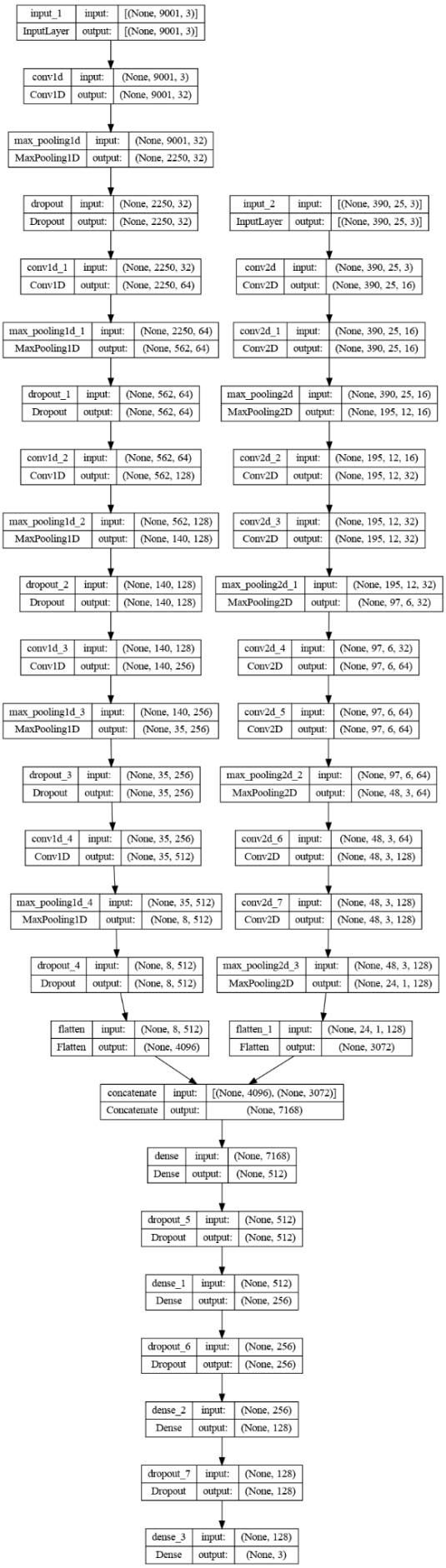
input_1 | input: | [(None, 9001, 3)]
InputLayer | output: | [(None, 9001, 3)]
conv1d | input: | (None, 9001, 3)
Conv1D | output: | (None, 9001, 32)
max_pooling1d | input: | (None, 9001, 32)
MaxPooling1D | output: | (None, 2250, 32)
dropout | input: | (None, 2250, 32)
Dropout | output: | (None, 2250, 32)
input_2 | input: | [(None, 390, 25, 3)]
InputLayer | output: | [(None, 390, 25, 3)]
conv1d_1 | input: | (None, 2250, 32)
Conv1D | output: | (None, 2250, 64)
conv2d | input: | (None, 390, 25, 3)
Conv2D | output: | (None, 390, 25, 16)
max_pooling1d_1 | input: | (None, 2250, 64)
MaxPooling1D | output: | (None, 562, 64)
conv2d_1 | input: | (None, 390, 25, 16)
Conv2D | output: | (None, 390, 25, 16)
dropout_1 | input: | (None, 562, 64)
Dropout | output: | (None, 562, 64)
max_pooling2d | input: | (None, 390, 25, 16)
MaxPooling2D | output: | (None, 195, 12, 16)
conv1d_2 | input: | (None, 562, 64)
Conv1D | output: | (None, 562, 128)
conv2d_2 | input: | (None, 195, 12, 16)
Conv2D | output: | (None, 195, 12, 32)
max_pooling1d_2 | input: | (None, 562, 128)
MaxPooling1D | output: | (None, 140, 128)
conv2d_3 | input: | (None, 195, 12, 32)
Conv2D | output: | (None, 195, 12, 32)
dropout_2 | input: | (None, 140, 128)
Dropout | output: | (None, 140, 128)
max_pooling2d_1 | input: | (None, 195, 12, 32)
MaxPooling2D | output: | (None, 97, 6, 32)
conv1d_3 | input: | (None, 140, 128)
Conv1D | output: | (None, 140, 256)
conv2d_4 | input: | (None, 97, 6, 32)
Conv2D | output: | (None, 97, 6, 64)
max_pooling1d_3 | input: | (None, 140, 256)
MaxPooling1D | output: | (None, 35, 256)
conv2d_5 | input: | (None, 97, 6, 64)
Conv2D | output: | (None, 97, 6, 64)
dropout_3 | input: | (None, 35, 256)
Dropout | output: | (None, 35, 256)
max_pooling2d_2 | input: | (None, 97, 6, 64)
MaxPooling2D | output: | (None, 48, 3, 64)
conv1d_4 | input: | (None, 35, 256)
Conv1D | output: | (None, 35, 512)
conv2d_6 | input: | (None, 48, 3, 64)
Conv2D | output: | (None, 48, 3, 128)
max_pooling1d_4 | input: | (None, 35, 512)
MaxPooling1D | output: | (None, 8, 512)
conv2d_7 | input: | (None, 48, 3, 128)
Conv2D | output: | (None, 48, 3, 128)
dropout_4 | input: | (None, 8, 512)
Dropout | output: | (None, 8, 512)
max_pooling2d_3 | input: | (None, 48, 3, 128)
MaxPooling2D | output: | (None, 24, 1, 128)
flatten | input: | (None, 8, 512)
Flatten | output: | (None, 4096)
flatten_1 | input: | (None, 24, 1, 128)
Flatten | output: | (None, 3072)
concatenate | input: | [(None, 4096), (None, 3072)]
Concatenate | output: | (None, 7168)
dense | input: | (None, 7168)
Dense | output: | (None, 512)
dropout_5 | input: | (None, 512)
Dropout | output: | (None, 512)
dense_1 | input: | (None, 512)
Dense | output: | (None, 256)
dropout_6 | input: | (None, 256)
Dropout | output: | (None, 256)
dense_2 | input: | (None, 256)
Dense | output: | (None, 128)
dropout_7 | input: | (None, 128)
Dropout | output: | (None, 128)
dense_3 | input: | (None, 128)
Dense | output: | (None, 3)

Figure S1: combined model architecture.

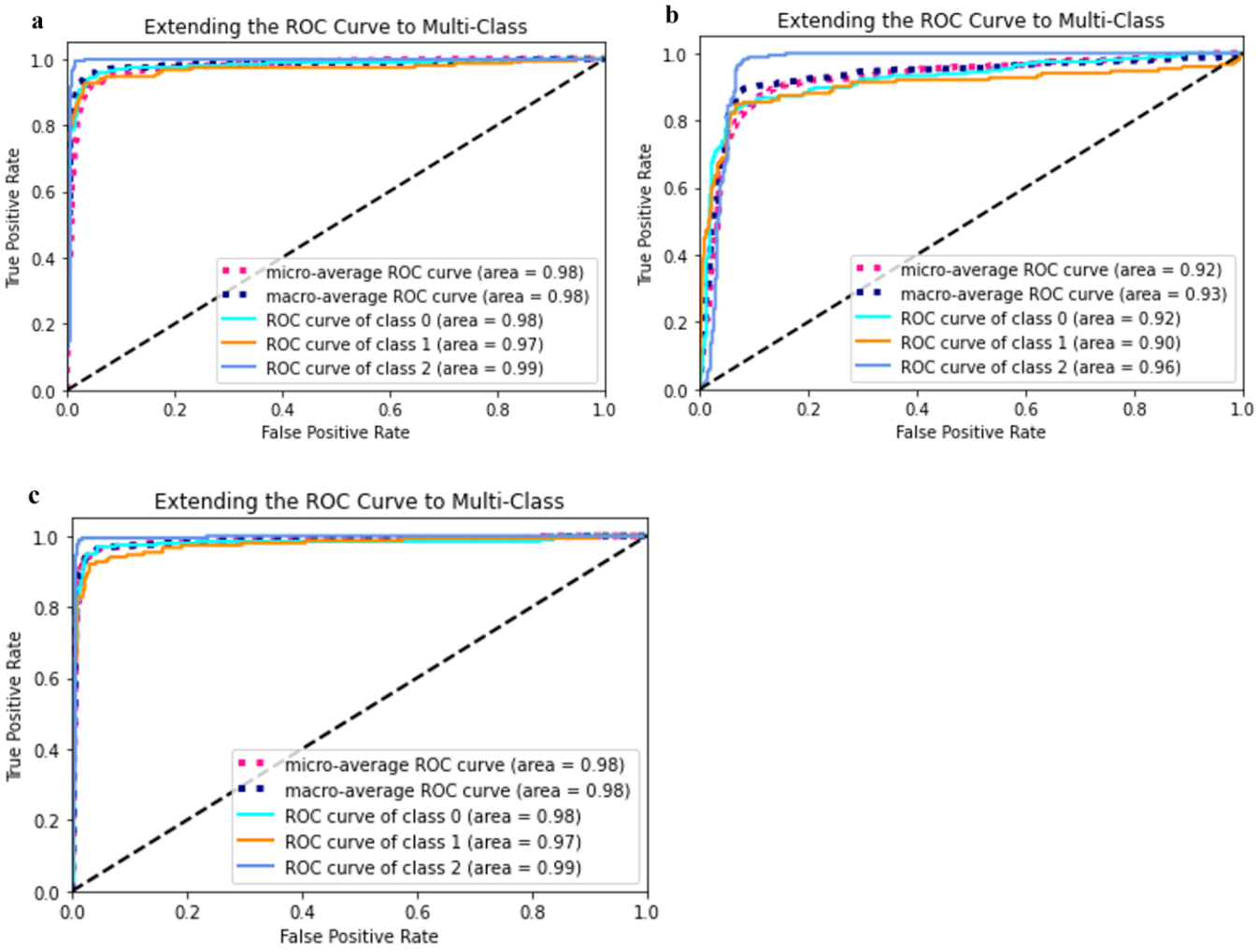

Figure S2: ROC plots of (A) Waveform model, (B) Spectrogram model and (C) Combined model.

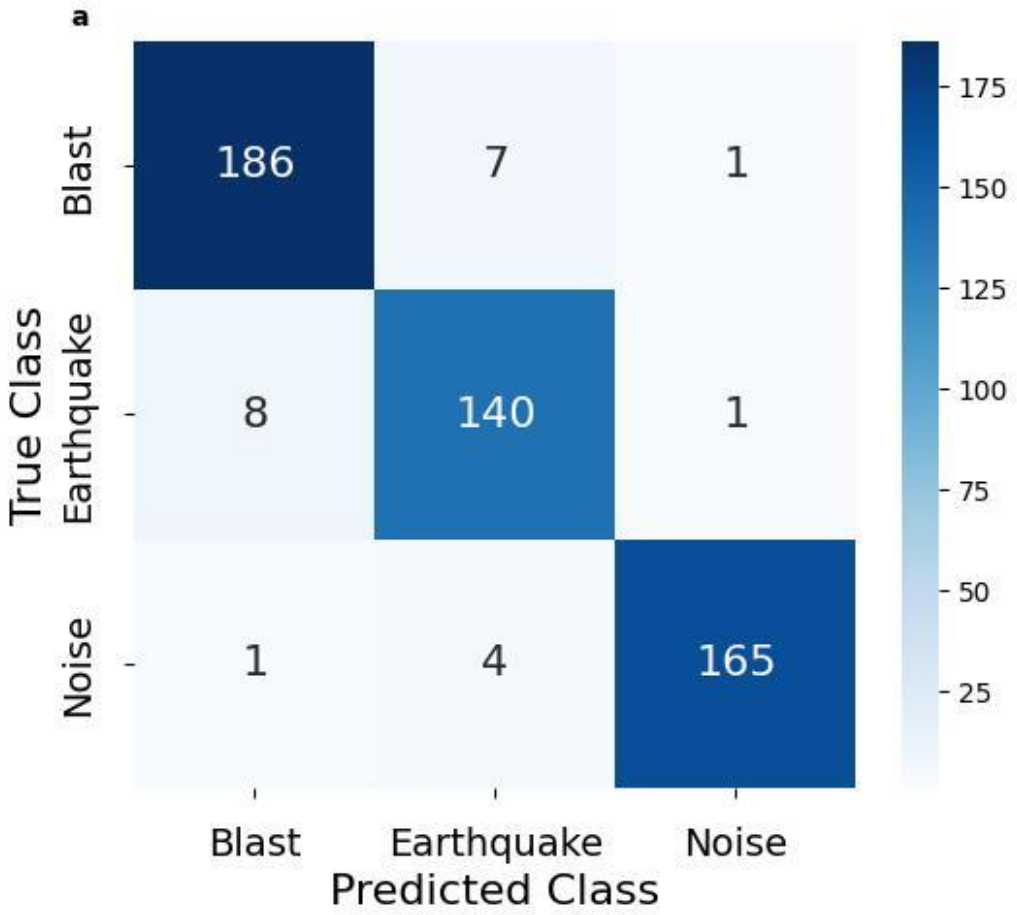
a
Blast
Earthquake
Noise
True Class
186
7
1
8
140
1
1
4
165
175
150
125
100
75
50
25
Blast
Earthquake
Noise
Predicted Class

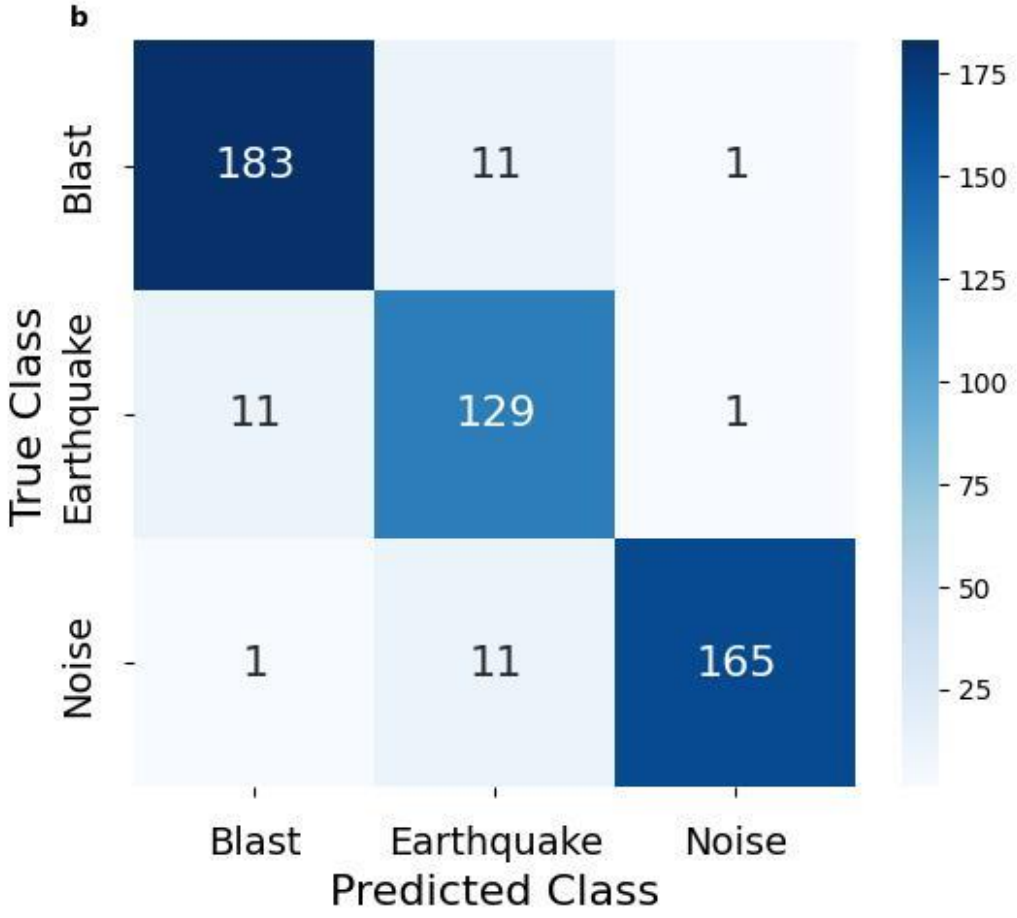
b
Blast
Earthquake
Noise
True Class
183
11
1
11
129
1
1
11
165
175
150
125
100
75
50
25
Blast
Earthquake
Noise
Predicted Class

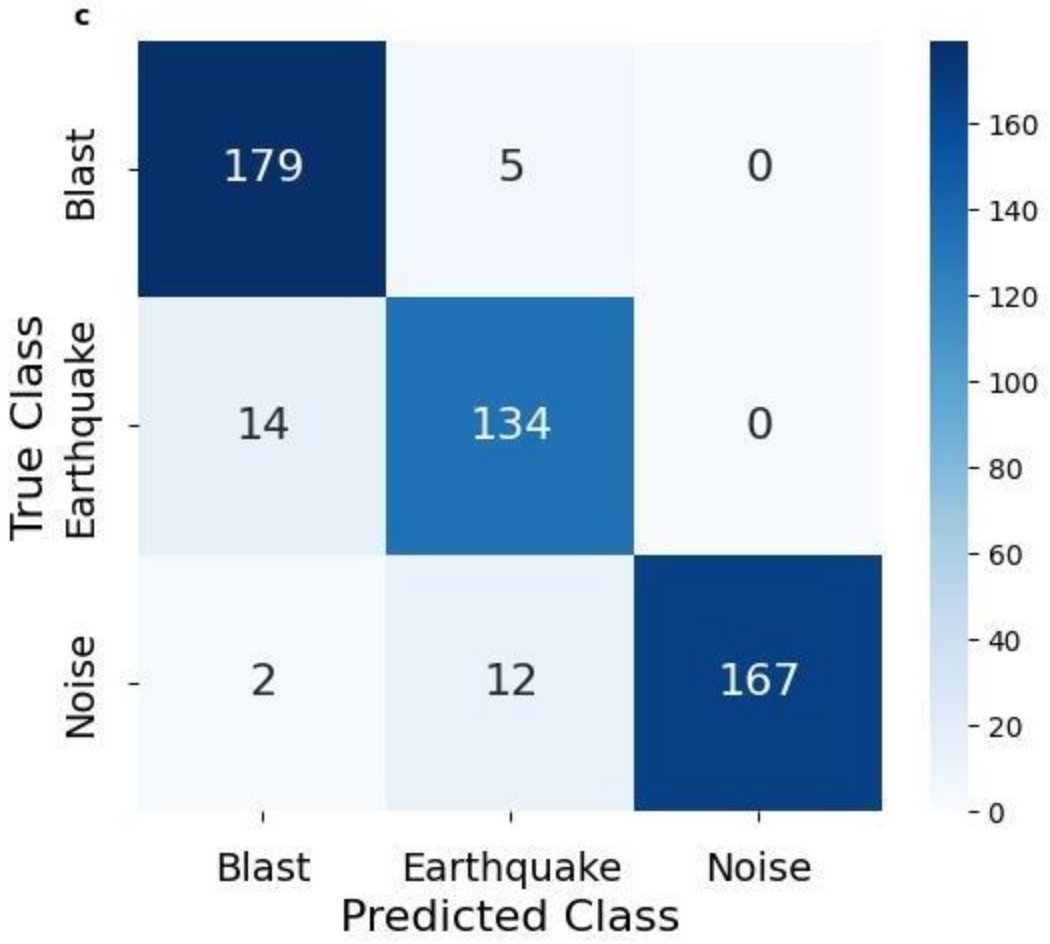

Fig. S3: Confusion matrices for analyzing and comparing the classification results obtained from three distinct models: (A) Waveform Model, (B) Spectrum Model, and (C) Combined Model.

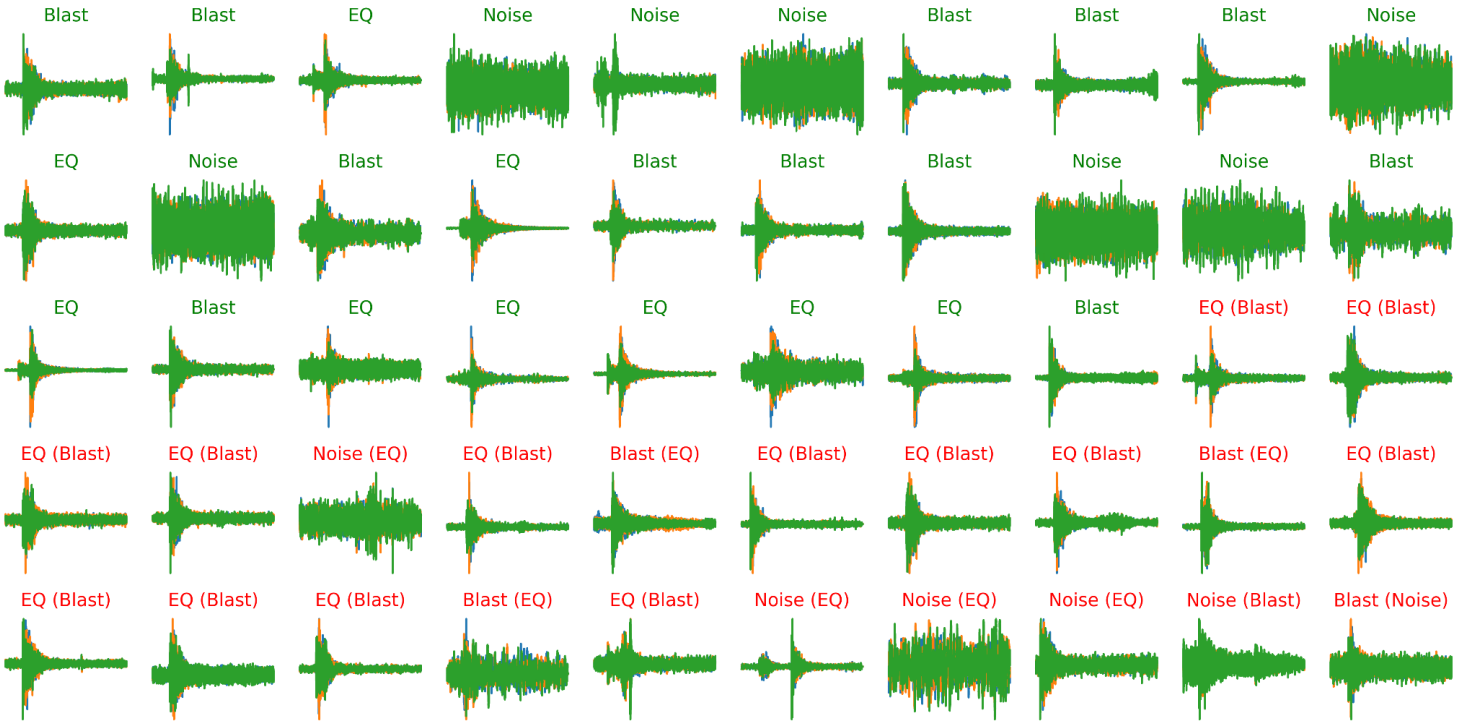

Figure S4: Visualization of test dataset traces along with their corresponding ground truth labels. The misclassified are shown in red colored font with the corresponding true labels in the brackets. It is evident that an increase in amplitude, especially when with poor signal-to-noise ratios led to classification errors.

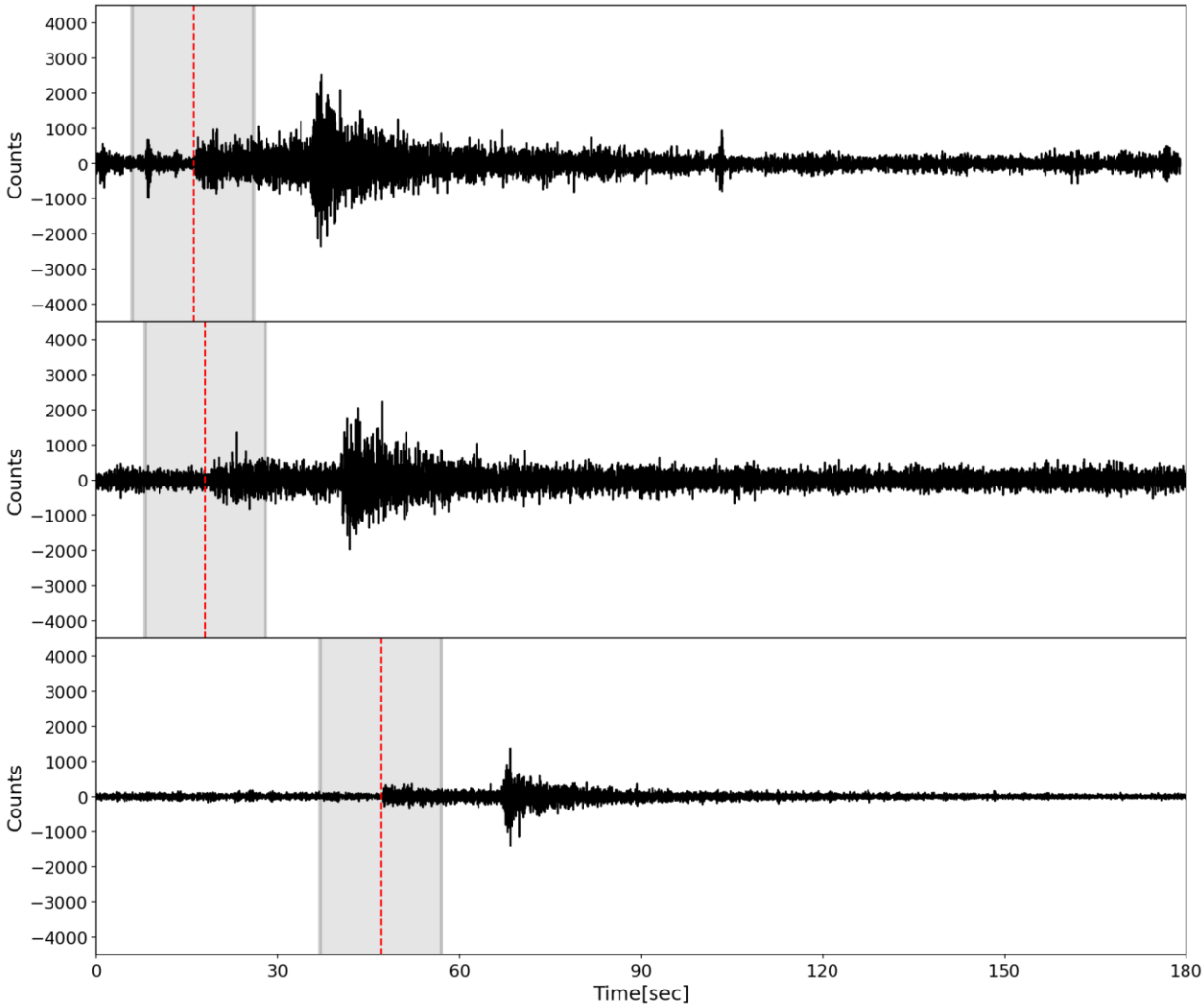

Figure S5: Examples of waveforms along with the selected window (gray shaded rectangle) to calculate the SNR. The dotted red line indicates the P phase, the shaded portion is a 20 s window, 10 s before and after P arrival each.

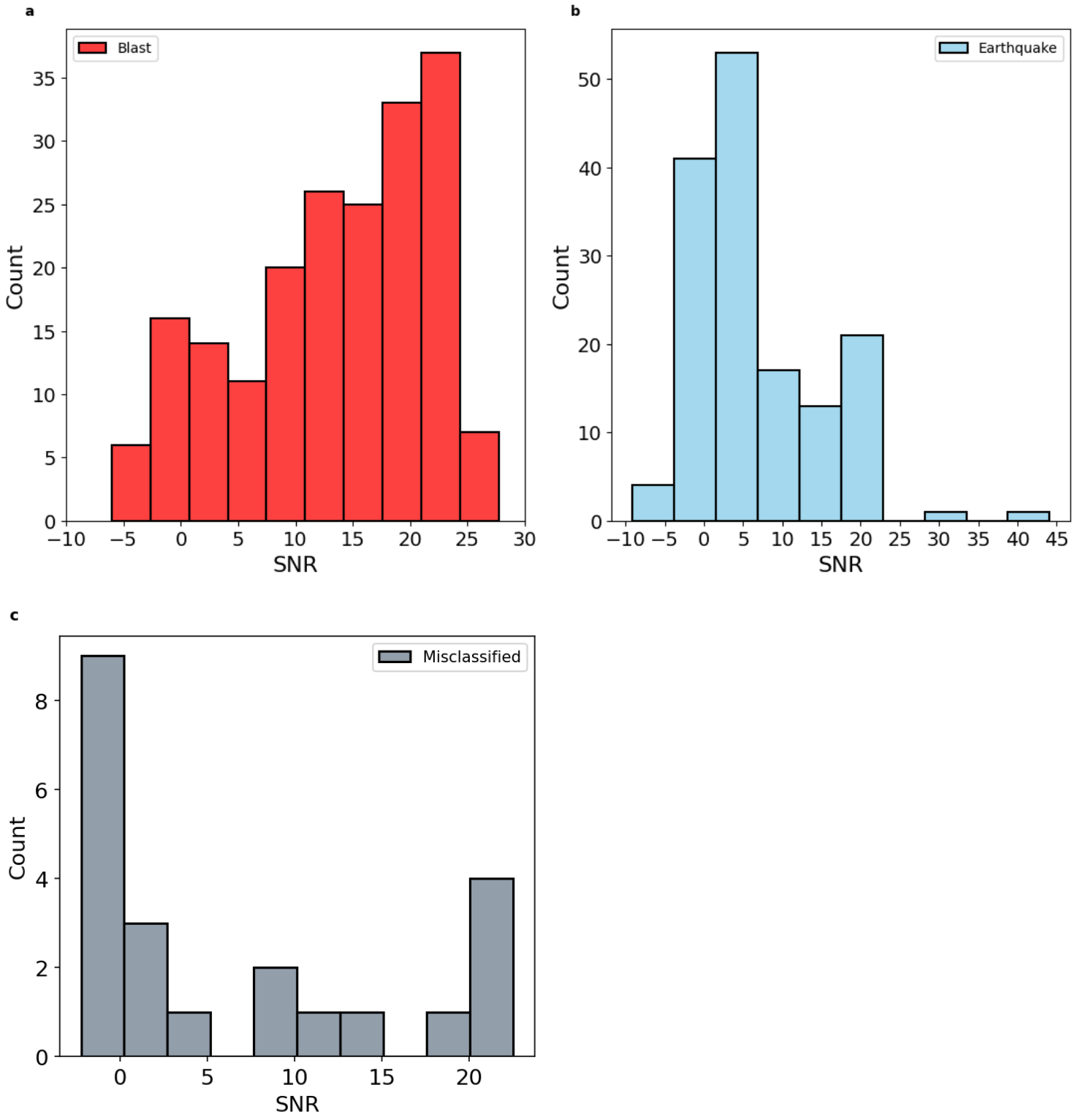

Figure S6: Signal-to-Noise Ratio of (a), (b), and (c) represents the SNR of blasts, earthquakes, and misclassified events, respectively, in the test dataset of the waveform model. When the strength of noise dominates over the signal,

i.e., $\left(\frac{\mu S^2}{\mu N^2}\right) < 1$, negative values are observed. The SNR of all the waveforms (earthquakes (151) and blasts (195)) varies from -9 to 44 dB, indicating that noise dominates over the signal.

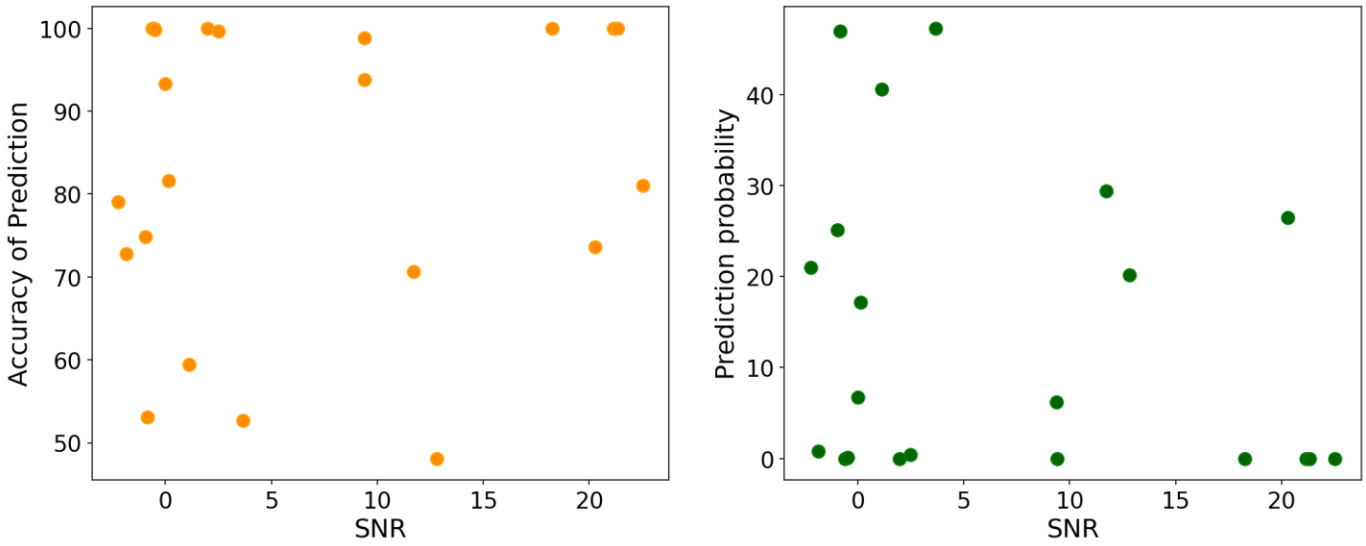

Figure S7: The figure shows the SNR values of the 22 misclassified events from the waveform model, along with the corresponding true (orange) and misclassified (green) prediction probabilities. The SNR is < 1 for 68% of the misclassified waveforms suggesting that the prediction probabilities for the true class are generally lower for misclassified waveforms with low SNR values.

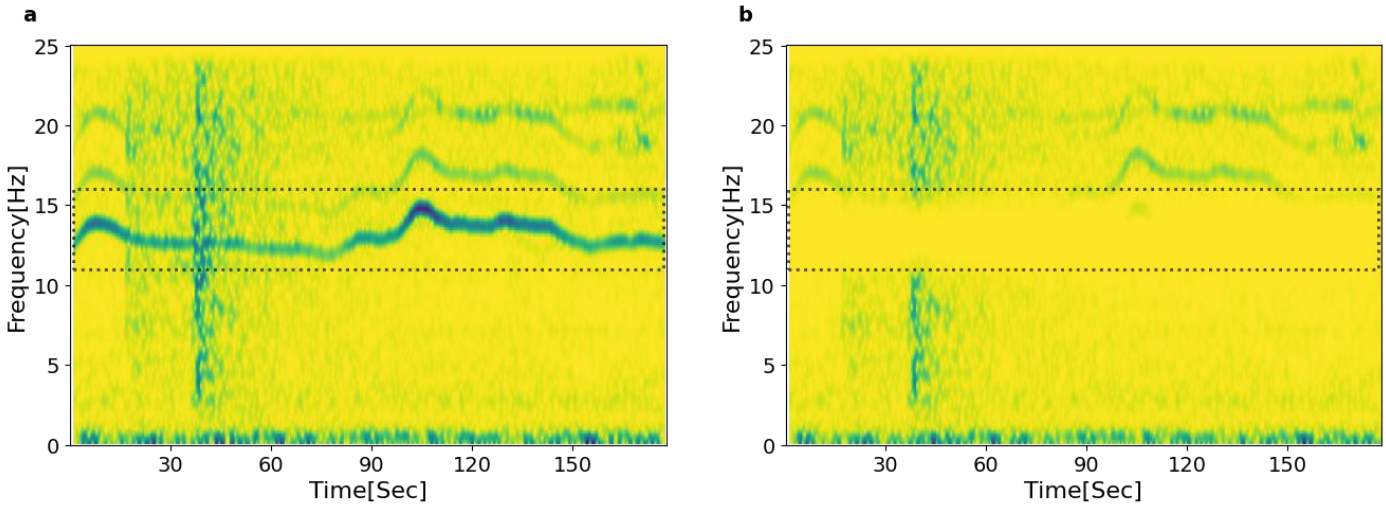

Figure S8: (a)Example of a misclassified spectrogram recorded at SUR station (on 2009-06-06 @ 10:27:42 GMT) showing three distinct energy bands within a frequency range through the selected time window. (b) Demonstrates the effect of applying a bandstop filter to attenuate these noise bands resulting in loss of information and a void at the filtered frequency band.

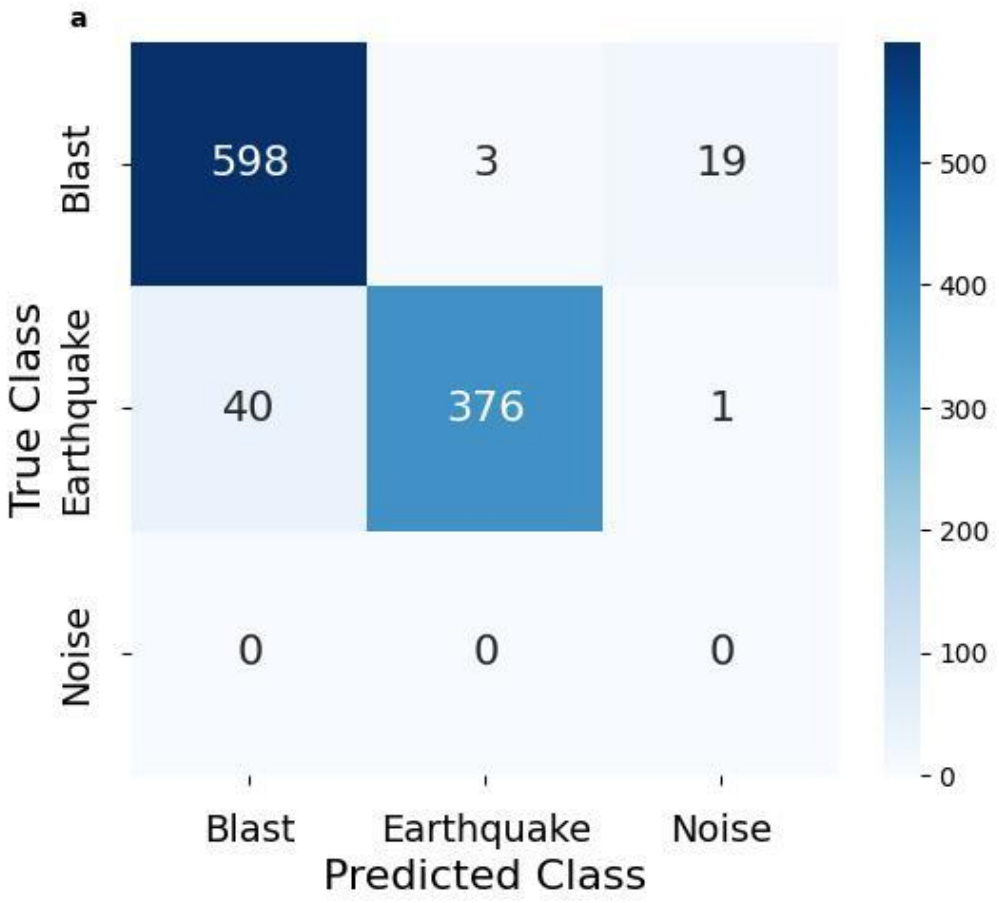
a
Blast
Earthquake
Noise
True Class
598
3
19
40
376
1
0
0
0
500
400
300
200
100
0
Blast
Earthquake
Noise
Predicted Class

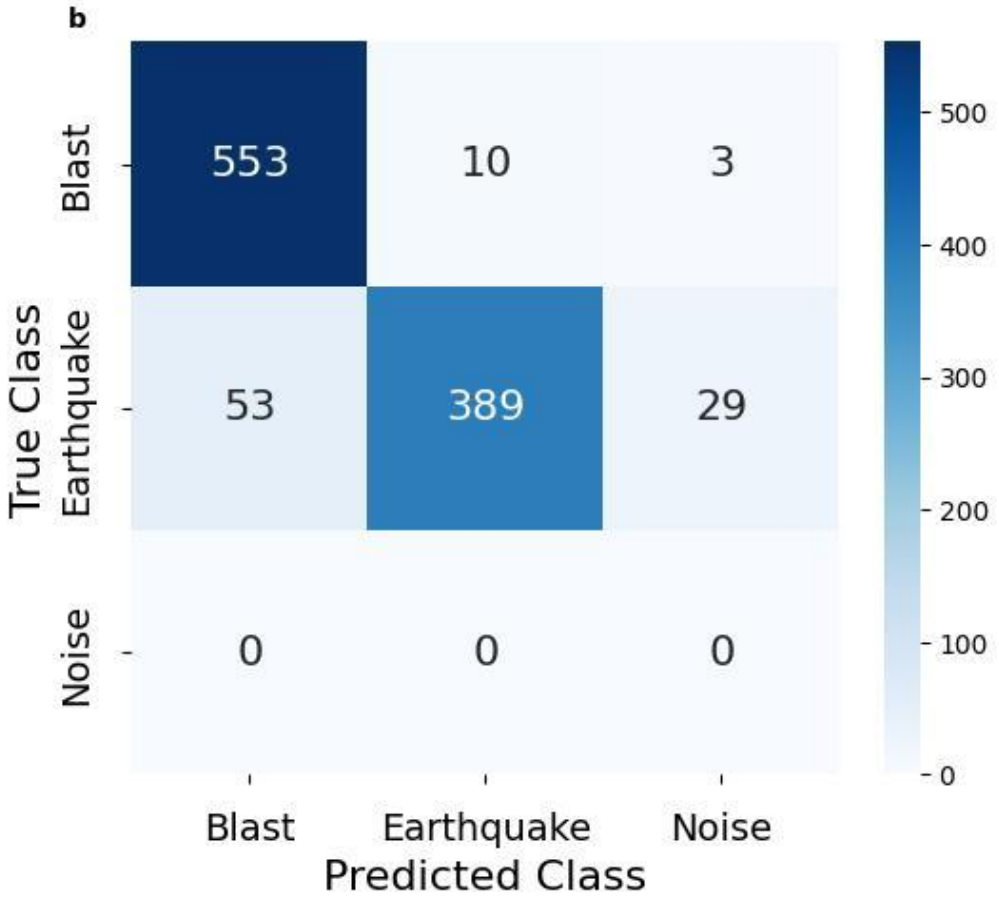
b
Blast
Earthquake
Noise
True Class
553
10
3
53
389
29
0
0
0
500
400
300
200
100
0
Blast
Earthquake
Noise
Predicted Class

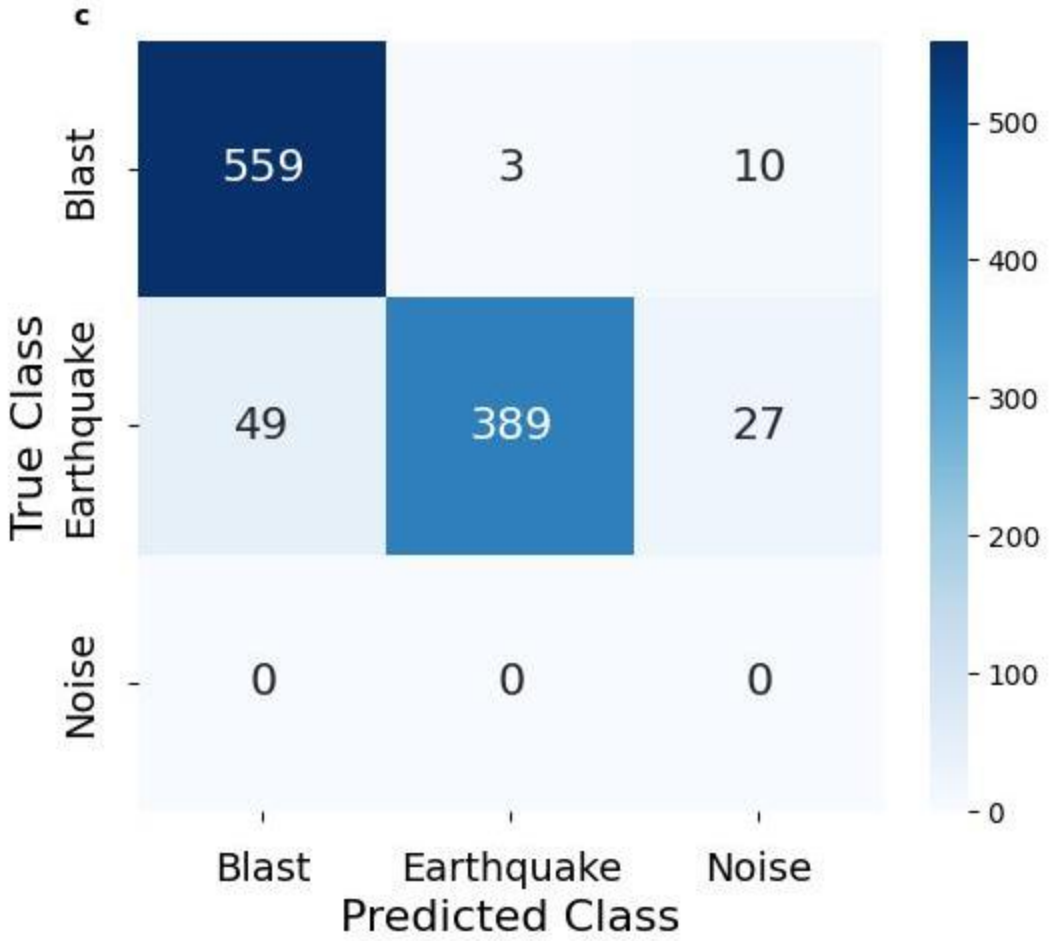

Fig S9: Confusion matrices for analyzing and comparing the classification results obtained from three distinct models: (a) Waveform Model, (b) Spectrum Model, and (c) Combined Model respectively when tested with data downloaded from SCEDC, on which the models are not trained.